10th European Conference on Turbomachinery
Fluid Dynamics and Thermodynamics
15-19 April 2013 – Lappeenranta, Finland

PERFORMANCE PREDICTION AND OPTIMIZATION OF LOW PRESSURE AXIAL FANS BY ARTIFICIAL NEURAL NETWORKS

K. Bamberger - T. Carolus

University of Siegen
Institute for Fluid- and Thermodynamics
Paul-Bonatz-Strasse 9-11
57068 Siegen, Germany
konrad.bamberger@uni-siegen.de

ABSTRACT

Reliable prediction of pressure rise and power demand of axial fans is a fundamental requirement in design and optimization processes. Moreover, prediction of the downstream velocity profile is needed for the design of guide vanes. Experimental tests and CFD simulations represent reliable, but costly methods. The aim of this work is to replace these methods by CFD-trained meta-models, or more specifically by artificial neural networks (ANNs). Aiming at a general purpose prediction tool, the input space was chosen such that high flexibility can be achieved with a limited number of physically interpretable parameters. Application of the ANNs to two sample fans showed good agreement with simulations and measurements. The usefulness of the validated ANNs was then illustrated by using them in parameter studies as well as in an optimization process revealing potentials for efficiency improvement and extension of operating range.

NOMENCLATURE

Latin symbols

A	area
D	diameter
P	power
R	regression
S	tip clearance
$\dot{V}$	volume flow rate
d	(max.) thickness of airfoil
f	(max.) camber of airfoil
n	rotational speed of fan
p	pressure
r	radius
u	circumferential speed of blade
x	coordinates along airfoil
z	Cartesian coordinate here: axis of rotation

Greek symbols

α	angle of attack
β	flow angle
γ	blade stagger angle
ϕ	flow coefficient
η	efficiency
λ	sweep angle
ρ	density
θ	angle of rotation
ψ	pressure coefficient

Abbreviations

ANN	artificial neural network
CFD	computational fluid dynamics
MLP	multilayer perceptron
RANS	Reynolds averaged Navier Stokes
RBF	radial basis function
SST	shear stress transport

Subscripts and Indices

1, 2	plane up-/downstream of the fan
m	meridional
n	normal
h	hub
r	radial
s	shroud
t	total
ts	total-to-static
tt	total-to-total
θ	circumferential

INTRODUCTION

The qualification of artificial neural networks (ANNs) in performance prediction and optimization of turbomachinery has been proven by several recent studies. The overview given here focuses on work that is most relevant for the present case, i.e. the utilization of ANNs in low pressure axial fans (comparatively low Reynolds numbers and almost incompressible flow).

Ghorbanian and Gholamrezaei (2008) [1] presented a comparison between several ANN types and their ability to predict compressor performance in terms of compression ratio and efficiency as a function of flow rate and rotational speed (alternatively flow rate as function of compression ratio and rotational speed). Good agreement of predicted and measured performance could be achieved by all network types tested, but the most commonly used type, the multilayer perceptron (MLP) network, was superior in terms of generalization, i.e. at operating points far off the closest measuring data. They showed that the ANN approach can decrease testing time, but the results were limited to one specific compressor and prototyping as well as network training would need to be repeated for different designs.

A more general approach was taken by Arnone et al. in 2009 [2] who predicted the pressure head and efficiency of a Kaplan turbine for variable operating conditions as well as variable geometrical parameters in terms of stagger angles at runner and guide vanes. The MLP network was trained by computational fluid dynamics (CFD). The agreement between ANN prediction and measurements was good and thus the network could be applied to optimize the runner-guide vane stagger correlation for all runner positions. However, the solution is still application-specific as only few of the generally available geometrical parameters were incorporated into the network model.

Further examples of CFD-trained ANNs in the field of turbomachinery exist. In 2011, Checcucci et al. [3] used such a network to obtain the response surface in a centrifugal pump optimization problem. The optimum regarding efficiency and good suction capability was found out of eleven geometrical parameters. Good agreement between predicted and measured performance was achieved. The selection of input parameters was more general as compared to the upper examples, but still many problem specific constraints, e.g. the specific pump speed, were considered.

The interesting approach of using inverse artificial neural networks (iANNs) to optimize the geometry of a turbine runner was presented by Flores et al. in 2010 [4]. The optimization was successful and the ANNs obtained showed excellent performance, but only four operational inputs were considered (flow rate, flow components in two directions, and angular velocity) and the input range covered only ±2 % of the initial values.

The computational inexpensiveness as compared to CFD simulations has made ANNs a popular tool for the response surface in optimization problems where the number of CFD simulations can be reduced if the ANN is trained by CFD and later used to compute the target function instead of direct computation of the target function by CFD. Examples covering both approaches can be found in the book “Optimization and Computational Fluid Dynamics” by Thévenin and Janiga (2008) [5]. The same reference was utilized for the programming of the evolutionary optimization algorithm mentioned later in this paper.

The attempt of the current work is to apply the ANN approach in the field of low pressure axial fans. The flexibility in potential fan designs is strongly increased as compared to the references above by incorporating more input parameters with a greater range. Besides integral values such as pressure rise and efficiency, the circumferentially averaged flow field downstream of the runner is modeled by ANNs as well. This information is of high importance for the design of guide vanes.

Before training the ANN, a decision must be made about the network type and size. Here, multilayer feed-forward networks (or multilayer perceptron, MLP) with two hidden layers, sigmoid hidden neurons, and linear output neurons were constructed with the Neural Network Toolbox of MATLAB®. The main advantages and drawbacks of this network type, especially as compared to radial basis function (RBF) networks, are discussed by Nelles [6]. High accuracy, smoothness, and

insensitivity to noise are, among others, good attributes that suggest the choice of MLPs whereas many of the drawbacks described, e.g. time consuming training, are considered less relevant for the present case. However, owing to the ridge construction method, no locality exists in MLPs. Locality describes the capability of ANNs to model processes within a strictly limited input space region which has no effect on other regions. In the present case, the lack of locality represents an important disadvantage in the incorporation of stall behavior into the model, which is overcome by using different networks for operating points in stall. Whether or not stall occurs is predicted by a pattern recognition network that has a similar structure as described above except that sigmoid transfer functions are also applied in the output layer. Optimization of the hidden layer weights is done by the Levenberg-Marquandt algorithm [7] and the conjugate gradient backpropagation method [8], respectively. Both methods belong to the class of nonlinear local optimization algorithms. The Levenberg-Marquandt algorithm is a powerful and fast method which has, however, drawbacks in large problems where the conjugate gradient method can be superior [6]. Network structure optimization (the number of neurons in each hidden layer) was done by a simple in-house algorithm based on the principle ideas of the steepest descent method.

The aim of this work is the construction of ANNs for low pressure axial fans predicting

- the pressure rise, Δp_{ts} and Δp_{tt},
- the power consumption P,
- the circumferentially averaged downstream velocity profile, $c_{m2}(r)$, $c_{\theta 2}(r)$, $c_{r2}(r)$.

Requirements for the input parameters are:

- provision of high geometrical flexibility,
- dimensionless where possible,
- physical interpretability.

The first point aims at general (not problem-specific) modeling of the fan performance. The latter two are required for informative conclusions from studies with the networks.

METHODOLOGY

Input Space

As outlined previously, the input parameters shall be dimensionless where possible. However, numerical simulations and testing must be conducted with real test objects wherefore at least the outer fan diameter, D, and the rotational speed, n, must be specified. Standard test conditions at the University of Siegen were selected, i.e. D = 0.3 m and n = 3000 min^{-1}. All other geometrical parameters can be referred to this diameter. Fixing D and n is not considered problematic because results for arbitrary combinations of D and n can be obtained by application of the well-known scaling laws

$$\Delta p \sim n^2 D^2 \rho \tag{1}$$

$$P \sim n^3 D^5 \tag{2}$$

$$c \sim \dot{V} \sim nD^3 \tag{3}$$

Taking into account varying Reynolds numbers may require scaling methods such as by Ackeret or more recently (2012) Pelz et al. [9]. The input parameters selected are similar to the design variables suggested by Carolus and Starzmann [10] in their work about axial fan design in 2011. This is supposed to ensure similar diversity of potential fan geometries as in state-of-the art design tools. Basic geometrical inputs are the hub-to-tip ratio (ν), the number of blades (z), and the tip clearance (S). One blade section is described by its chord length (c), sweep angle (λ), maximum camber/thickness (f, d) and position of maximum camber/thickness (x_f, x_d) of the utilized NACA sections. The reason for the choice of NACA sections is the high level of geometrical flexibility provided by only few parameters. The way the section geometry is constructed from these parameters and the impact on lift or drag of isolated airfoils can be found in the book “Theory of Wing Sec-

tions" by Abbot and Doenhoff [11]. Each of the values describing the sections is defined at hub, mid-span, and shroud with second degree polynomial interpolation in between. The angle of attack (α) is also varied along the span, but with five equally distributed sampling points. For the geometrical construction of the fan, the stagger angle is required. It is defined by

$$\gamma(r) = \beta_1(r) + \alpha(r), \text{ where} \tag{4}$$

$$\beta_1(r) = tan^{-1}\left(\frac{u_1(r)}{c_{m1}}\right) \text{ and } c_{m1} = \frac{\dot{V}_{design}}{A_1} = \frac{\phi_{design} \cdot \left(\pi^2/4\, nD^3\right)}{A_1} \tag{5}$$

As a consequence of that, the dimensionless design flow rate (ϕ_{design}) represents a further input parameter which is also required for incorporation of the sweep angle (λ). In principle, it is also possible to use the stagger angle as input parameter instead of the angle of attack. This option has the advantage that purely geometrical parameters would be used. However, a large range of potential stagger angles would need to be considered whereas the angle of attack can be restricted to a comparatively low range which avoids extreme fluctuations between different spanwise locations. Moreover, more realistic designs can be expected by consideration of the spanwise distribution of the inlet flow angle β_1. The sweep angle is defined as the angle between the incoming relative velocity $w_1(r, \phi_{design})$ and the blade stacking line which goes through the center of gravity of each section. Details about the blade construction incorporating a sweep angle as well as its aerodynamic and acoustic effect are discussed by Beiler and Carolus (1999) [12].

The actual flow rate (ϕ) may differ from the design flow rate and represents the last input parameter. A graphical illustration of all geometrical input parameters is depicted in Figure 1. All input parameters as well as their definitions and ranges are listed in Table 1.

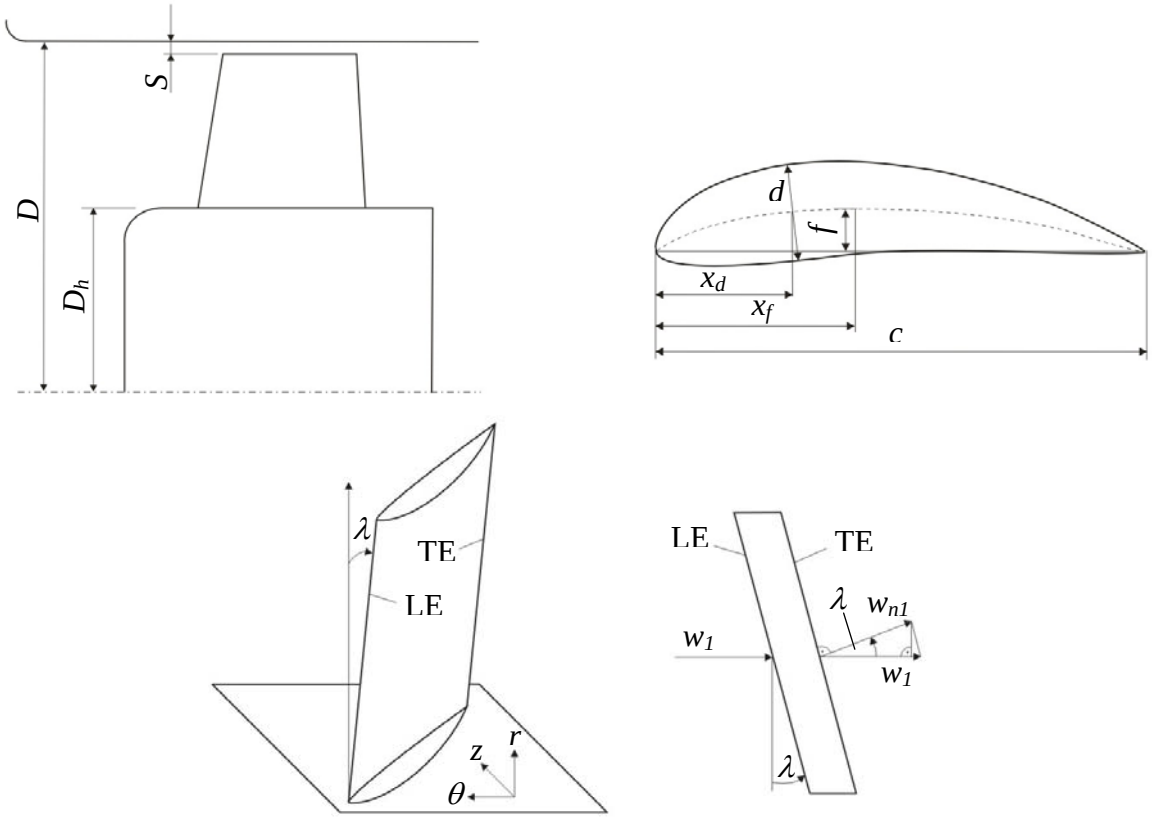

Figure 1: Illustration of geometrical input parameters. Top left: Side view of a fan in a duct. Top right: Blade section. Bottom: Definition of the blade sweep angle in a 3D and 2D view (here: constant sweep angle from hub to shroud).

Training Data Generation

Training data for the ANNs was generated by random variation of the input parameters and evaluation of the target values by means of CFD. The rotating computational domain was discretized with the commercial grid generator ANSYS TurboGrid® 14.0. The grid is block-structured and contains approx. 500,000 hexahedral elements complying with the grid quality specifications defined in the ANSYS user manuals. The domain extends one fan diameter upstream and two fan diameters downstream of the fan blade. A general grid interface (GGI) was placed in the tip clearance. To save computational time, only one blade passage, with periodic boundary conditions at the sides, was simulated. Further boundary conditions are rotational speed, given mass flow rate at the inlet, ambient pressure at the outlet and no slip at the walls (hub, shroud, and blade). The Reynolds number varies with flow rate and fan geometry. A typical value is around 200,000. The Reynolds-Averaged Navier-Stokes (RANS) equations were solved with ANSYS CFX® 14.0. Usage of a steady state CFD model is inevitable for reasons of computational cost, but increases the uncertainty in stall regions where the flow field is highly transient. The resulting impact on network performance will be discussed in the subsequent sections. The selected turbulence model is shear stress transport (SST) and the iteration limit is 200. Solutions that fail a specific residual target are sorted out to avoid too much noise in ANN training data. However, these considerations must always be balanced against the demand for covering the input space as much as possible. A good tradeoff between these two requirements was found to be that solutions with residuals higher than 10^{-1} MAX or fluctuations of integral target values (e.g. Δp, P) higher than 10% within the last 20 iterations are excluded from the training data. The pressure was evaluated at planes placed ½ fan radius upstream of the leading edge or downstream of the trailing edge, respectively. In the downstream plane, the velocity field was circumferentially averaged in CFX POST® 14.0 and the values at 100 equally spaced points in the radial direction were captured in the result data as well. This procedure was automated by replay scripts and more than 5,000 simulations were conducted with parallelization on 20 CPUs (5 parallel simulations, each on 4 CPUs). The total computational effort amounts to approx. $1.1 \cdot 10^4$ CPU hours.

Table 1: Definition and ranges of input parameters.

Name	Symbol/Definition	Range	Comment
Hub-to-tip ratio	$\nu = D_h / D$	0.3 – 0.6	
Number of blades	z	5 – 11	Only integers
Tip clearance ratio	S / D	0.0005 – 0.005	
Chord length ratio	c / D	0.133 – 0.333	
Rel. max. camber[1]	f / c	0 – 0.09	NACA section
Rel. position of max. camber[1]	x_f / c	0.1 – 0.8	NACA section
Rel. max. thickness[1]	d / c	0.05 – 0.15	NACA section
Rel. position of max. thickness[1]	x_d / c	0.1 – 0.7	NACA section
Angle of attack[2]	α	-5° – +15°	Against w_1 vector
Sweep angle[1]	λ	-60° – +60°	Against w_1 vector
Design flow rate	ϕ_{design}	0.2 – 0.4	Required for γ and λ
Operating flow rate	ϕ	0.1 – 0.4	

[1] At three equally spaced radial positions with polynomial interpolation in between.

[2] At five equally spaced radial positions with polynomial interpolation in between.

ANN Construction

All networks were constructed and optimized with the Neural Network Toolbox of MATLAB®. A pattern recognition ANN was used to find ϕ_{stall} indicating stall for $\phi < \phi_{stall}$ and no stall for $\phi > \phi_{stall}$ where the criterion for stall was a negative mean value of c_{r1}. This empiric criterion was de-

rived from several simulations of complete characteristic performance curves (among others the upcoming curves in the result section). However, a criterion based on purely physical considerations is sought within the scope of further investigations. The pattern recognition network was trained with the complete training data using the conjugate gradient backpropagation optimization method to determine the hidden layer, output layer, and bias weights. The training data was then split into two categories (stall or not) and a total of twelve MLP networks were trained to predict Δp_{ts}, Δp_{tt}, P, c_{m2}, $c_{\theta 2}$, and c_{r2} for operating points in or not in stall using the Levenberg-Marquandt algorithm. The cost function for both optimization methods is the mean-square error between the network outputs and the target values. The actual training process was conducted with only 70% of the corresponding training data while 15% was used for both, validation and testing. Validation is required to stop training before over-fitting occurs while testing is required to check the ANN performance with data that in no way contributed to the optimization process. A closer discussion of over-fitting is given by Nelles [6]. The optimal network structure was obtained by initially constructing networks with ten neurons in each of the two hidden layers and increasing/decreasing the number of neurons in the most promising direction. Only the performance in the test data was considered for the comparison of network structures.

The c_2 ANNs have 34 output neurons, corresponding to 34 points that are evenly distributed in radial direction, where the velocity was evaluated. Utilization of more points immensely increases the network construction time, but is feasible with the training data gathered.

Dimensionless values for the ANN outputs were not used because the efficiency tends to (minus) infinity when P approaches 0 (Δp_{tt} being negative then). However, dimensionless values can be obtained by

$$\psi = \frac{\Delta p}{\pi/4\, n^2 D^2 \rho} \quad (\rho = 1.185 \text{ kg/m}^3 \text{ throughout the simulations}) \text{ and} \tag{6}$$

$$\eta = \frac{\dot{V} \Delta p}{P} \tag{7}$$

Experimental Set-Up

Characteristic curves were measured at the chamber test rig of the University of Siegen according to DIN 24163 [13]. The accuracy in ψ_{ts} and η_{ts} is high, but no total-to-total values can directly be measured. Velocities downstream of the fan were measured using either hot-wire anemometry or a five-hole probe. The reason for two different measuring techniques was that the ANNs were validated against measurements with two pre-existing fans of which one velocity profile obtained from hot-wire anemometry was already known. The new measurements for this work were done using the five-hole probe. Both techniques yield a measuring tolerance lower than ±5% of the measuring value.

Results

Network performance

Figure 2 compares the ANN output data with the targets (CFD results) for the most important networks meaning that c_{r2}, which is always comparatively low and less relevant for the design of guide vanes, and Δp_{tt}, which cannot be measured and is often unnecessary in practice, are spared. Only the test data, i.e. data that was not used for the network training, is plotted. It can be seen that good agreement between output and target can be achieved, especially in ANNs for operating conditions without stall. With an ideal ANN, all points would perfectly match the straight curve in each plot, resulting in a regression value $R = 1$. Some of the actual values given on each plot get quite close to that. The minimum value occurs at the $c_{\theta 2}$ prediction under stall conditions, with $R_{min} = 0.865$. However, excellent agreement in stall was not expected as under those operating conditions

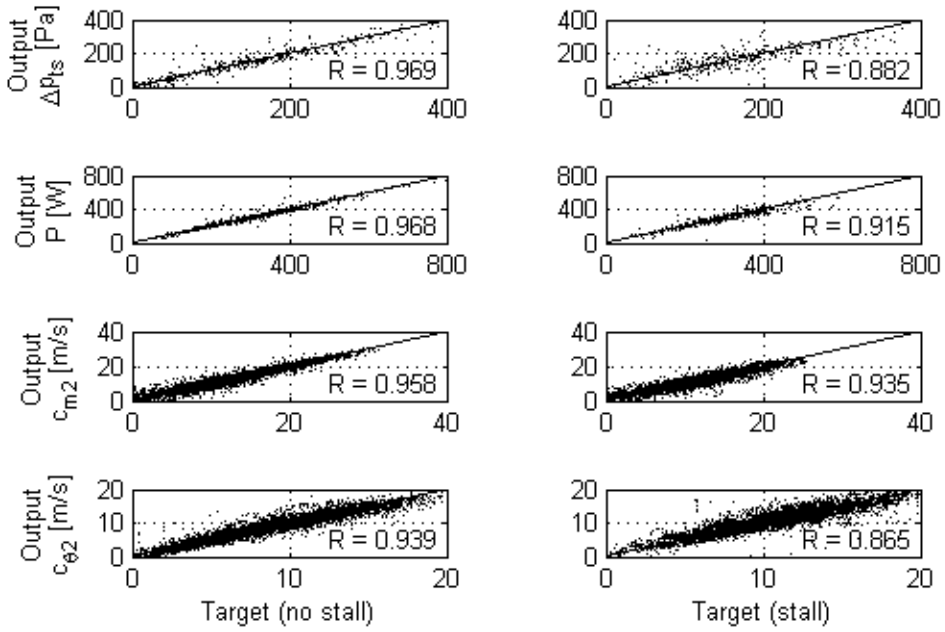

Figure 2: Output over target for selected ANNs. The target values are the CFD results and have the same dimension as the respective input.

the flow becomes unstable and unsteady, wherefore steady state CFD simulations do not provide accurate results increasing the noise in the network training. Whether or not stall occurs is predicted correctly in 95.1% of the test cases. Table 2 lists the optimal network structures and regression values found by the structure optimization.

Table 2: Optimal network structures and regression values of test data.

Network	Size of hidden layers (no stall)	Size of hidden layers (at stall)	Regression (no stall)	Regression (at stall)
Δp_{ts}	11 x 10	11 x 11	0.9686	0.8821
Δp_{tt}	9 x 10	11 x 10	0.9535	0.8330
P	12 x 12	11 x 11	0.9680	0.9150
c_{m2}	10 x 10	12 x 12	0.9584	0.9349
$c_{\theta 2}$	9 x 11	8 x 13	0.9393	0.8646
c_{r2}	9 x 10	10 x 11	0.7719	0.6105

The ANNs were then applied to compute complete characteristic curves of two fans designed at the University of Siegen. Both fans were designed with the blade element method (BEM) as suggested by Carolus [14] or Carolus and Starzmann [10] and are known from earlier investigations by Kohlhaas et al. [15] and Sturm et. al [16]. The ANN validation with these two fans appears adequate because of their quite different design. The first fan has six thick unswept blades and a rather large hub-to-tip ratio. In contrast, the second fan has five thin swept blades and a rather small hub-to-tip ratio. The operating rage is quite different, as it can be seen on the following plots. The only similarities are x_f and x_d of the airfoil sections used.

A comparison of ANN-predicted, CFD-simulated and measured curves is shown in Figure 3. Comparisons between CFD and experiment can be used to assess the adequacy of the numerical model to predict fan curves and consequently its adequacy to be used for the ANN training. Comparisons between ANN and CFD are suitable to asses the ANN ability to substitute CFD simulations

Direct comparisons between ANN and measurement are not useful as good agreement can also originate from cancelling out of ANN and CFD errors. The stall flow rate, ϕ_{stall}, is predicted with high precision by both, ANN and CFD in case of Fan 1 but has a minor offset in case of Fan 2. The pressure curves and efficiency curves are matched with reasonable accuracy, too. In Figure 4, a similar comparison is depicted for the downstream velocity components c_{m2} and $c_{\theta 2}$ at the respective design points. Again, good agreement of ANN, CFD, and measurements is achieved.

After the successful validation, the usefulness of the ANNs shall be shown by conducting a parameter study as well as an optimization. In the parameter study, blade sweep within a range of ±40° is applied to the previously unswept Fan 1 and the capability to delay stall is examined. The sweep angle is defined at hub and shroud only, while their mean value is used at midspan.

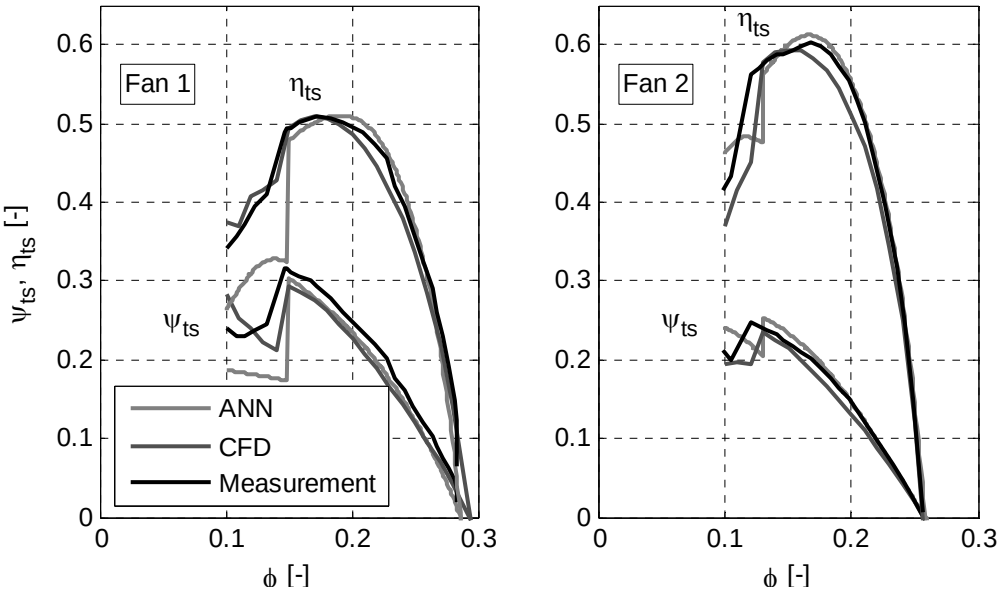

Figure 3: Comparison of ANN, CFD, and experiments regarding pressure rise and efficiency.

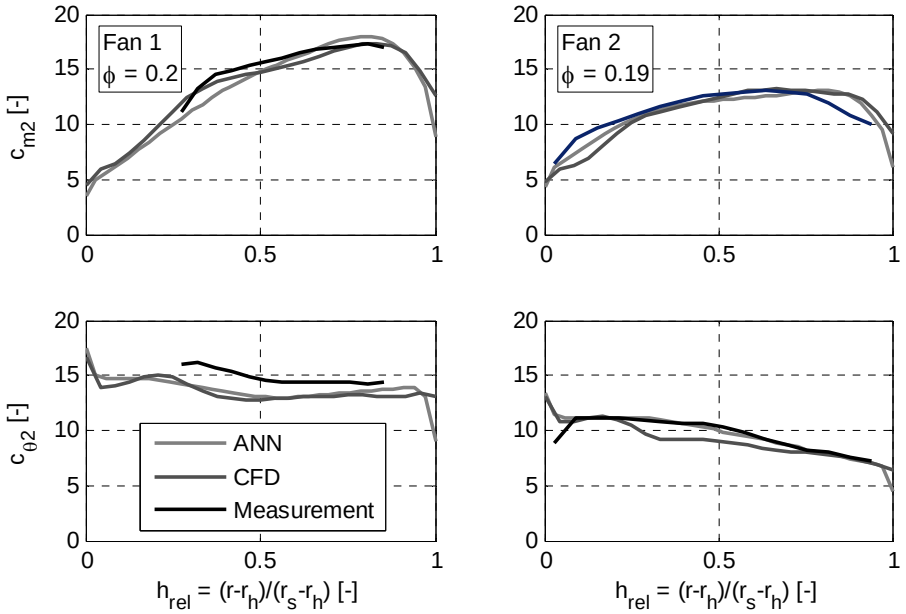

Figure 4: Comparison of ANN, CFD, and experiments regarding c_2 components at design point.

Figure 5 illustrates that positive sweep angles can delay stall considerably. Moreover, the characteristic curve of the promising configuration $\lambda_h = \lambda_s = 40°$ is computed and compared with the original Fan 1. It is found that the sweep angle decreases blade lift resulting in lower pressure rise and total-to-static efficiency for $\phi > \phi_{stall}$. This has been discussed in detail by Beiler [17] and is often compensated by increasing the chord length.

In the case study demonstrating an optimization, only the camber (f and x_f) of Fan 2 was varied while all other input parameters were kept constant. The target function of the evolutionary optimization algorithm was the total-to-static efficiency at mostly unchanged pressure curve. The resulting characteristic curves are depicted in Figure 6 and reveal a successful optimization. Blade load has been shifted away from the tip region towards lower blade sections, especially towards midspan. This is also illustrated by the c_2 curves on the right side. No aerodynamic explanation is sought here as the focus is on ANN training, validation and application.

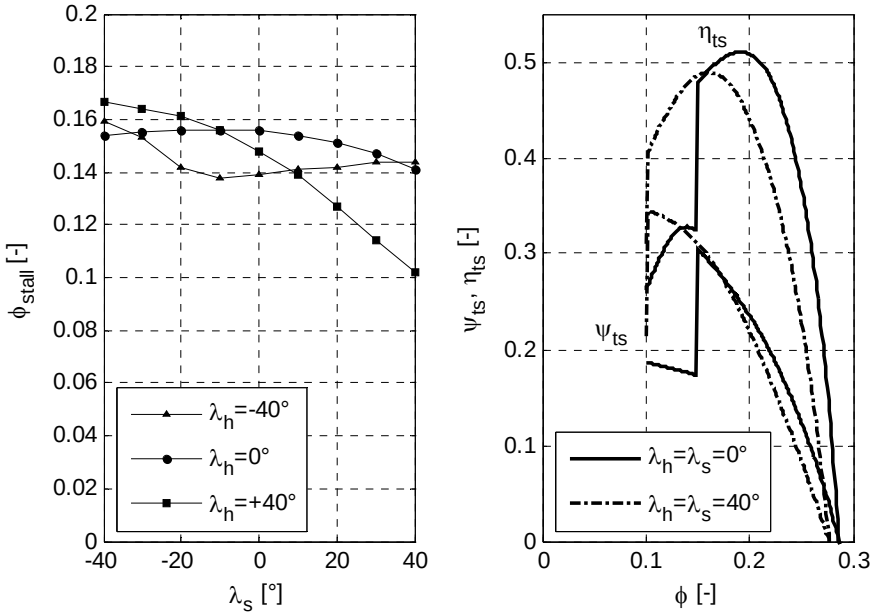

Figure 5: Results from blade sweep variation (Fan 1). Left: Impact of blade sweep on stall point. Right: Characteristic curves with and without sweep.

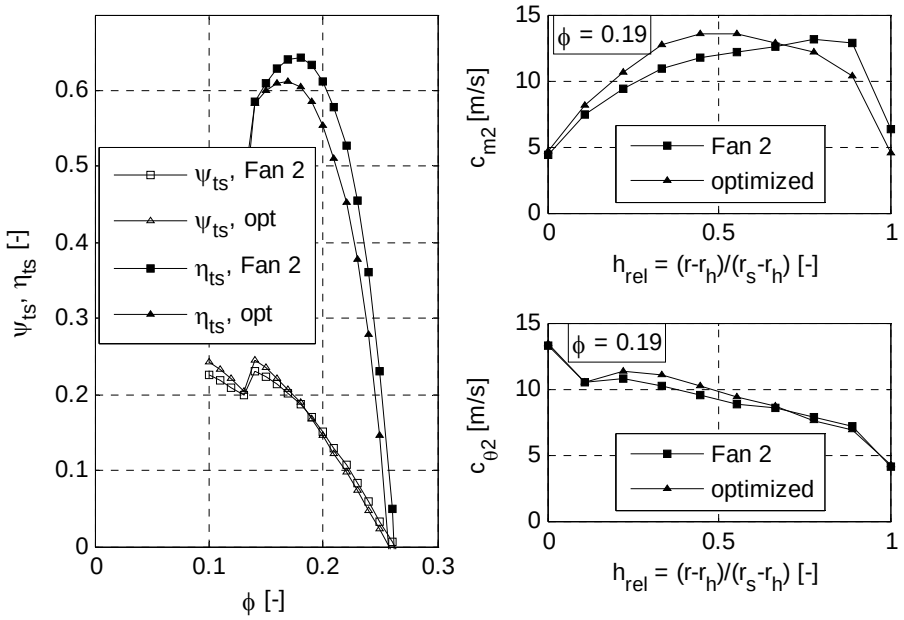

Figure 6: Impact of η_{ts}-optimization on characteristic curves and downstream flow field at the design point ϕ = 0.19.

CONCLUSIONS

Previous experience with ANNs in the field of turbomachinery was transferred to the specific application on low pressure axial fans. A set of ANNs predicting the stall point, pressure rise, power consumption, and circumferentially averaged downstream flow field was constructed. The ANNs were trained by steady state CFD data, validated, and applied. The input layer comprises 28 geometrical and operational parameters and thus is considerably extended as compared to previous studies resulting in a general purpose prediction tool. It could be shown that the optimization of the network structure and the layer weights allows the construction of ANNs with high accuracy. Validation against CFD-simulated as well as experimentally measured characteristic fan curves of two sample fans showed good agreement. This also applies to the comparison of downstream velocities obtained from these three techniques. Agreement between CFD and experiments proves the adequacy of the numerical model for the network training while the agreement between ANN and CFD proves sufficient training of the network. Examples for the exploitation of the ANNs were given by their application in a parameter study as well as in an optimization which yielded the potential to delay stall by incorporation of blade sweep and the potential to improve efficiency by optimized blade sections, respectively. Results from these ANN studies were obtained by several orders of magnitude quicker than it would have been possible with comparable CFD studies. No aerodynamic explanation for the improved performance is sought within the scope of this work as the focus is on ANN methodology.

Future work will focus on both, further validation and application of the ANNs. Additional validation work is required for extraordinary designs, e.g. far off in Cordier's diagram of optimal turbomachinery stages. Despite quite different shapes, the two sample fans used in this work were both designed with a similar philosophy. For example, their design points are typical for axial fans and the blade sections were selected according to promising 2D airfoil polars. After the successful validation, the ANNs will offer a valuable design tool for operating points where strong 3D flow effects prohibit using the blade element method. The qualification to work in these regions was already indicated by the precise prediction of the stall point, but it was also shown that some precision is lost beyond this point. It should be examined to which extent the accuracy can be improved by further training. However, it will always be limited to the performance of RANS simulations which on principle deliver uncertain results for flows with strongly unsteady behavior.

The further exploitation of ANNs in parameter studies and optimization algorithms can be used to scrutinize general assumptions in fan design methods, to develop design recommendations, or simply as a fan design tool. The usage in optimization problems will also detect weak points of the ANNs as the optimizer will always find regions with unrealistically high performance predictions.

REFERENCES

[1] Ghorbanian, K., Gholamrezaei, M. (2009) – *An Artificial Neural Network Approach to Compressor Performance Prediction*. Applied Energy 86, pp. 1210-1221

[2] Arnone, A., Marconcini, M., Rubechini F., Schneider A., Alba G.. (2009) – *An Kaplan Turbine Performance Prediction Using CFD: An Artificial Neural Network Approach.* Proceedings: International Conference and Exhibition, Lyon, France

[3] Checcucci, M., Sazzini, F., Marconcini, M., Arnone, A., Coneri, M., De Franco, L., Toselli, M. (2011) – *Assessment of a Neural Network Based Optimization Tool. A Low Specific Speed Impeller Application.* International Journal of Rotating Machinery 2011, Article ID 817547

[4] Flores, J., Urquiza, G.., Hernández, J., (2010) – *Inverse Neural Network to Optimal Performance of the Hydraulic Turbine Runner Blades*. International Journal of Advancements in Computing Technology 2, No 4

[5] Thévenin, D., Janiga, G.. (2008) – *Optimization and Computational Fluid Dynamics*. Heidelberg: Springer Verlag GmbH

[6] Nelles, O. (2001) – *Nonlinear System Identification*. Heidelberg: Springer Verlag GmbH

[7] Marquardt, D. (1963). *An Algorithm for Least-Squares Estimation of Nonlinear Parameters.* SIAM Journal on Applied Mathematics 11, pp. 431–441

[8] Straeter, T (1971). – *On the Extension of the Davidon-Broyden Class of Rank One, Quasi-Newton Minimization Methods to an Infinite Dimensional Hilbert Space with Applications to Optimal Control Problems*. NASA Technical Reports Server

[9] Pelz, P., Stonjek, S, Matyschok, B. (2012) – *The Influence of Reynolds Number and Roughness on the Efficiency of Axial and Centrifugal Fans - a physically based scaling method*. Fan2012, Senlis, France

[10] Carolus, T., Starzmann , R. (2011) – *An Aerodynamic Design Methodology for Low Pressure Axial Fans with integrated Airfoil Polar Prediction*. Proceedings of the ASME Turbo Expo 2011, Vancouver, Canada

[11] Abbot, I., von Doenhoff, A (1959). – *Theory of Wing Sections*. New York: Dover Publications Inc.

[12] Beiler, M., Carolus T. (1999) – *Computation and Measurement of the Flow in Axial Flow Fans With Skewed Blades*. Journal of Turbomachinery 121, pp. 59-66

[13] DIN 24163 (1985) – *Fans; Performance Testing, Standard Characteristics*. Deutsche Norm, Berlin

[14] Carolus, T. (2009) - *Ventilatoren - Aerodynamischer Entwurf, Schallvorhersage, Konstruktion (2. Auflage)*. Wiesbaden: B. G. Teubner / GWV Fachverlage GmbH

[15] Kohlhaas, M., Carolus, T. (2012) – *Trailing Edge Blowing for Reduction of Rotor-Stator Interaction Noise: Criteria, Design and Measurements.* ISROMAC-14, Honolulu, USA

[16] Sturm, M., Carolus, T. (2012) – Tonal Fan Noise of an Isolated Axial Fan Rotor due to Inhomogeneous Coherent Structures at the Intake. Fan2012, Senlis, France

[17] Beiler, M. (1996) – *Untersuchung der dreidimensionalen Strömung durch Axialventilatoren mit gekrümmten Schaufeln*. Düsseldorf: VDI Verlag GmbH